Mem. S.A.It. Vol. 85, 84

Memorie della

Probing μ with H_2 absorption lines at $z_{abs} \simeq 2.66$ toward Q J 0643−5041 with VLT-UVES

H. Rahmani[1], D. Albornoz Vásquez[2], R. Srianand[1], P. Petitjean[2], P. Noterdaeme[2], and C. Ledoux[3]

[1] Inter-University Centre for Astronomy and Astrophysics, Post Bag 4, Ganeshkhind, Pune 411 007, India
[2] Institut d'Astrophysique de Paris, UMR 7095 CNRS, Université Pierre et Marie Curie, 98 bis Boulevard Arago, Paris 75014, France
[3] European Southern Observatory, Alonso de Córdova 3107, Casilla 19001, Vitacura, Santiago, Chile

Abstract. Molecular hydrogen in the interstellar medium (ISM) of high redshift galaxies can be detected directly from its UV absorption imprinted in the spectrum of background quasars. Given the numerous H_2 lines usually detected, these absorption systems are unique tools to constrain the cosmological variation of the proton-to-electron mass ratio, μ. We intend to derive a useful constraint on the variation of μ using high signal-to-noise ratio, high-resolution VLT-UVES data of Q J 0643−5041 amounting to a total of more than 23 hours exposure time, and fitting the H_2 absorption features with multiple-component Voigt profiles. We follow the procedures used in our previous works to derive a constraint on the cosmological variation of μ, $\Delta\mu/\mu = (7.3 \pm 4.3_{stat} \pm 4.1_{syst}) \times 10^{-6}$.

Key words. galaxies: ISM – quasars: absorption lines – quasars: individuals: Q J 0643−5041 – cosmology: observations

1. Introduction

Molecular hydrogen is observed in damped Lyman-α (DLA) systems. These are spectral absorption features of large neutral hydrogen (H I) column densities ($N(\mathrm{H\,I}) \geq 2\times10^{20}$ cm^{-2}) found in the line of sight of quasars. More easily formed, and shielded from UV radiation, in dusty environments, H_2 is detected at $z > 1.8$ via Lyman- and Werner-band absorption lines in about 10% of the DLAs down to molecular fractions of $f = 2N(H_2)/(2N(H_2) + N(\mathrm{H\,I})) \sim 10^{-4.5}$ (Noterdaeme et al. 2008).

Grand Unified Theories predict the variation of the fundamental parameter $\mu = m_p/m_e$, the proton-to-electron mass ratio. Thompson (1975) proposed to probe μ in astrophysical absorbing systems by comparing the measured wavelengths of identified ro-vibrational transitions of molecules to their vacuum laboratory-established values. Relative shifts between different line positions can be translated into $\mu_{abs} \neq \mu_{lab}$, where μ_{lab} is the laboratory measured value[1] and μ_{abs} is its value at z_{abs}. Variation of μ has been constrained using H_2 in 7 H_2-bearing DLAs at $z > 2$, suggesting that $\Delta\mu/\mu < 10^{-5}$ at $2 < z < 3$ (with $\Delta\mu/\mu \equiv$

[1] In the laboratory: $\mu_{lab} = m_p/m_e \simeq 1836.1526675(39)$ (Mohr & Taylor 2000).

$(\mu_z - \mu_0)/\mu_0$ where μ_z and μ_0 are the values of μ at redshift z and today).

We present our analysis of H_2 absorption features in the $z_{\rm abs}$ = 2.6586 DLA towards Q J 0643−5041 using VLT-UVES observations. We treat the data with extreme care and search for subtle systematic effects possibly introducing wavelength shifts. We make use of the numerous H_2 transitions detected to derive a robust limit on $\Delta\mu/\mu$. More details on this work can be found in Albornoz Vásquez et al. (2013).

2. Observations and data processing

The detection of H_2 at $z_{\rm abs}$= 2.66 towards Q 0643−5041 ($z_{\rm em}$ = 3.09) was first reported in Noterdaeme et al. (2008). This quasar was observed using both spectroscopic VLT-UVES arms (Dekker et al. 2000) in 2003 and 2004 in the course of programs IDs 072.A-0442(A) (aimed to study DLAs, PI S. López), 073.A-0071(A) (aimed to search for H_2-bearing systems at high redshift, PI C. Ledoux) and 074.A-0201(A) (aimed to constrain the variation of the fine-structure constant at high redshift using metal absorption lines, PI R. Srianand). There was no ThAr lamp attached to these observations. D'Odorico et al. (2000) have shown that the resetting of the grating between an object exposure and the ThAr calibration lamp exposure can result in an error of the order of a few hundred meters per second in the wavelength calibration. To minimize such errors, we only use more recent (2007-2008) data, namely, from program ID 080.A-0228(A) aimed to constrain the cosmological variation of μ (PI P. Petitjean). The setting for all the exposures was a 1 arcsec slit and 2×2 binning of the CCD pixels, for achieving a resolving power of $R \sim 45000$ or $FWHM \sim 6.7$ km s^{-1} in the blue arm. Wavelength calibration was performed with attached ThAr exposures. We further exclude the exposure with 1389 seconds of EXPTIME (10th row of Table 1 in Albornoz Vásquez et al. 2013) as the quality of this spectrum is very poor. Therefore, the combined spectrum to be used for μ measurement is made of 14 exposures with SNR of between 11 – 31 over our wavelength range of interest.

The data was reduced using UVES Common Pipeline Library (CPL) data reduction pipeline release 5.3.11[2] using the optimal extraction method, with 4th order polynomials to find the dispersion solutions. The number of suitable ThAr lines used for wavelength calibration was usually more than 700 and the rms error was found to be in the range 70–80 m s^{-1} with zero average. However, this error reflects only the calibration error at the observed wavelengths of the ThAr lines that are used for wavelength calibration. To combine the exposures we start from the final unrebinned extracted spectrum of each order produced by the CPL. We apply the CPL wavelength solution to each order and merge the orders by implementing a weighted mean in the overlapping regions. In the last step we made use of an uniform wavelength array of step size of 2.0 km s^{-1} for all exposures. As a result no further rebinning is required for spectrum combination. We fitted a continuum to each individual spectrum and generated a combined spectrum using a weighted mean. We further fit a lower order polynomial to adjust the continuum. In Rahmani et al. (2013) we found this procedure to produce final combined spectrum consistent with that obtained using UVES_POPLER.

Due to the shortcomings of the ThAr calibration of VLT/UVES spectra, we follow the method of Rahmani et al. (2013) and perform a cross-correlation analysis between the combined spectrum and the individual exposures to estimate the offset between them over the wavelength range of echelle orders of the blue arm. We observe that EXP5 (see Table 1 in Albornoz Vásquez et al. 2013) has the maximum constant offset of $\lesssim$ 300 m s^{-1}, while other exposures show constant offsets consistent with zero shift. We correct the measured shifts for individual orders of each exposure and make a new combined spectrum, and subsequently analyse its impact on $\Delta\mu/\mu$. We have checked the stability of the spectra over a one-month period of observations by making two combined spectra of EXP7 – EXP14 and

[2] http://www.eso.org/sci/facilities/paranal/instruments/uves/doc

EXP17 – EXP20, and, apart from a constant shift of $\sim 80\,\mathrm{m\,s^{-1}}$, no clear wavelength dependent systematic is seen. Rahmani et al. (2013) compared the asteroids spectra from UVES and the solar spectrum to discover a wavelength dependent systematic error in UVES observations. Moreover, they showed that such systematics can mimic a $\Delta\mu/\mu$ in the range of 2.5 – 13.7 ppm which is changing in different epochs from 2010 to 2012. Such a systematic cannot be revealed from the cross-correlation analysis between the individual exposures and the combined spectrum of this quasar, i.e. without a reference spectrum. Unfortunately we do not have asteroids observations with the same settings of and close in time to our science observations, hence we are not in a position to check whether such a drift is present in our data.

We verify the instrumental zero flux level of the spectra, bearing in mind that UVES is not flux calibrated, by studying the noise at the bottom of saturated Lyman-α-forest lines, associated with large scale gas clouds in the intergalactic medium which are extended enough to cover the background source completely. Indeed, QSOs are compact objects emitting an intrinsic and extremely luminous continuum flux. Broad emission lines seen in the spectra of quasars are believed to originate from an extended parsec scale region, the broad line region (BLR). Balashev et al. (2011) reported that an intervening molecular cloud toward Q1232+082 covers only a fraction of the BLR, most probably because of its compact size. This results in a residual flux detected at the bottom of saturated spectral features associated with the neutral cloud at wavelengths that are coincident with the BLR emission. Albornoz Vásquez et al. (2013) discussed a similar effect in the line of sight of Q 0643−5041, translated into a residual flux at the bottom of saturated H_2 lines of the molecular cloud at $z_{\rm abs}$= 2.6586 toward Q 0643−5041. However, the effect amounts only to $\simeq 4\%$ of the total flux, and is not exactly coincident with the weak BLR lines that we could identify, as it is also the case in Balashev et al. (2011). Therefore, we cannot attempt to correct this effect, and its influence on the precise determination of the H_2 features is unknown, but most probably very small.

H_2 is detected in a single component up to rotational level $J = 5$, with mild evidence for the presence of $J = 6$ and 7, at the same position as C I. Low ionization metals show a broader profile with more than 20 components. However, the molecular component is the dustiest (see Albornoz Vásquez et al. 2013).

3. Constraining the cosmic variation of μ

We use the intervening H_2 absorption lines seen in the spectrum of Q 0643−5041 to measure $\Delta\mu/\mu$. The sensitivity of the wavelength of the i'th H_2 transition to the variation of μ is generally parametrised as

$$\lambda_i = \lambda_i^0 (1 + z_{\rm abs})\Big(1 + K_i \frac{\Delta\mu}{\mu}\Big), \qquad (1)$$

where λ_i^0 is the rest frame wavelength of the transition, λ_i is the observed wavelength, K_i is the sensitivity coefficient of i'th transition, given by $K_i = {\rm d}\ln\lambda_{\rm i}^0/{\rm d}\ln\mu$ and $z_{\rm abs}$ is the redshift of the H_2 system. Here we use the most recent data on K_i given by Ubachs (2007) and the rest wavelengths and oscillator strengths from Malec et al. (2010). Eq. 1 can be rearranged as

$$z_i = z_{\rm abs} + CK_i, \qquad C = (1 + z_{\rm abs})\frac{\Delta\mu}{\mu} \qquad (2)$$

which clearly shows that $z_{\rm abs}$ is only the mean redshift of transitions with $K_i = 0$. z_i is the redshift of the i'th H_2 transition. Eq. 2 is sometimes presented as

$$z_{red} \equiv \frac{(z_i - z_{abs})}{(1 + z_{abs})} = K_i \frac{\Delta\mu}{\mu} \qquad (3)$$

which shows that the value of $\Delta\mu/\mu$ can be determined using the reduced redshift (z_{red}) versus K_i.

Like in Rahmani et al. (2013) we use two approaches to measure $\Delta\mu/\mu$. In the first approach we fit the H_2 lines using single velocity component and estimate the redshift for each H_2 transition, and measure $\Delta\mu/\mu$ using Eq. 3.

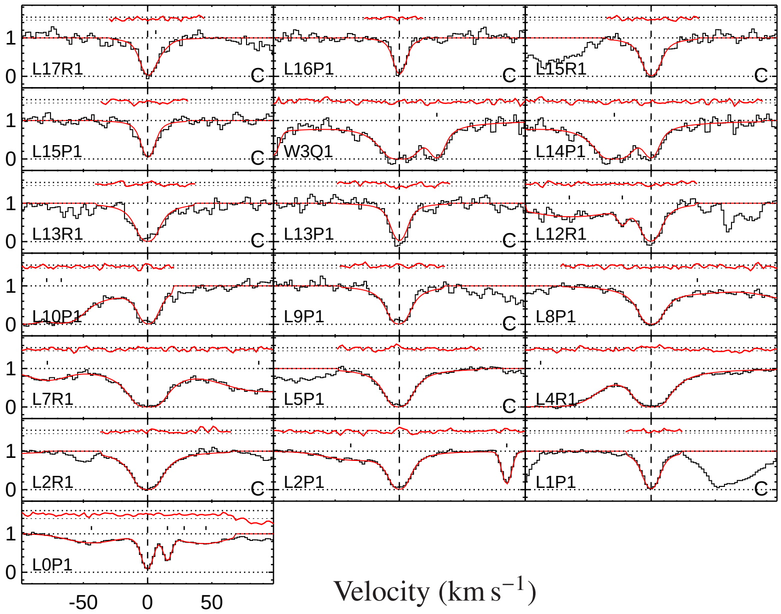

Fig. 1. Absorption profile of H_2 transitions from the $J = 1$ level and the best-fitting Voigt profile. The normalized residual (i.e. ([data]−[model])/[error]) for each fit is also shown in the top of each panel along with the 1σ line. We present the clean absorption lines by putting a letter "C" in the right bottom of these transitions.

In the second approach we explicitly use $\Delta\mu/\mu$ as one of the fitting parameters in addition to N, b and z in VPFIT. This approach allows for a multi-component fit of the H_2 lines. The results of $\Delta\mu/\mu$ for various approaches are given in Table 1.

To carry out a measurement of μ we need to choose a suitable set of H_2 lines. Although H_2 absorption from high J-levels (J = 4 – 7) are detected toward Q 0643−5041, they are too weak to lead to very accurate redshift measurements, as required for this study. Therefore, we reject H_2 lines from these high-J levels while measuring $\Delta\mu/\mu$, and only use H_2 absorption from J = 0 – 3. By carefully inspecting the combined spectrum we identified 81 lines suitable for $\Delta\mu/\mu$ measurements. 38 out of 81 lines are mildly blended with the intervening Lyman-α absorption of the intergalactic medium. We accurately model surrounding contaminations using multi-component Voigt-profile fitting, while simultaneously fitting the H_2 lines (see Fig. 1). A list of H_2 transitions we used is tabulated in Table B in Albornoz Vásquez et al. (2013), where clean lines are highlighted.

4. Results

Most measurements of $\Delta\mu/\mu$ using H_2 use the measured slope between the reduced redshifts and K_i. The most important step in this approach is to measure the redshifts and associated errors of a set of chosen H_2 absorption lines. To measure the redshifts of the suitable H_2 lines we first choose a model in which all the J-levels have the same b parameter. The best fitted model in this case has a reduced χ^2 ($\chi^2_{\rm red}$) of 1.57, the main contribution to it being the underestimation of the flux error rather than a poor Voigt profile model. A z-vs-K analysis of the fitted redshifts based on a linear regression gives $\Delta\mu/\mu$ = (5.0 ± 6.1) ppm. The quoted error is obtained using the bootstrap technique. The physical study of this H_2 system (Albornoz Vásquez et al. 2013) and also other H_2 systems (see Noterdaeme et al. 2007)

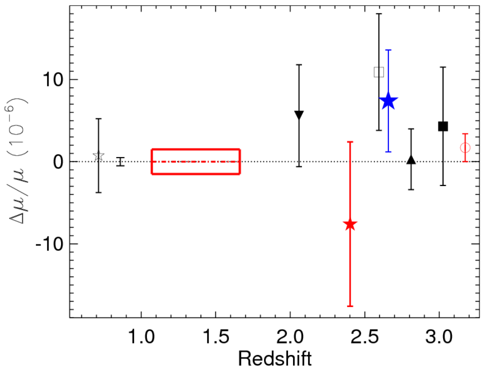

Fig. 2. Comparing $\Delta\mu/\mu$ measurement in this work and those in the literature. All measurements at 2.0 < z < 3.1 are based on the analysis of H_2 absorption. The filled larger blue star shows our result and the smaller red star shows the result from Rahmani et al. (2013). The downwards filled triangle is $\Delta\mu/\mu$ measurement from Malec et al. (2010). The filled upward triangle and the empty and filled squares are respectively from King et al. (2011), King et al. (2008) and Wendt & Molaro (2012). The solid box and the open circle present the constraint obtained respectively by Rahmani et al. (2012) and Srianand et al. (2010) based on the comparison between 21-cm and metal lines in Mg II absorbers under the assumption that α and g_p have not varied. The $\Delta\mu/\mu$ at z < 1 are based on ammonia and methanol inversion transitions that their 5σ errors are shown. The measurement at $z \sim 0.89$ is from Bagdonaite et al. (2013). The $\Delta\mu/\mu$ at $z \sim 0.684$ is from Murphy et al. (2008).

shows that different J-levels may bear different turbulent parameters. In particular, J = 0 and 1 lines have smaller b-parameters compared to higher J-levels. Hence we define a second model in which different J-levels are allowed to have different b-parameters. The best such fitted model has a $\chi^2_{\rm red}$ = 1.55. The z-vs-K analysis out of these fitted redshifts yields $\Delta\mu/\mu$ = (4.6 ± 5.9) ppm. Applying the above discussed models on the shift-corrected combined spectrum we find $\Delta\mu/\mu$ of (8.1±6.6) ppm and (7.6 ± 6.4) ppm for tied and untied b, respectively. While being consistent both values are ~ 3 ppm larger in comparison with the uncorrected ones.

Next, we include $\Delta\mu/\mu$ as a parameter of the fits. In these fits we also estimate the corrected Akaike information criteria (AICC) as given in Eq. 4 of King et al. (2011), and scale the statistical error of $\Delta\mu/\mu$ by the corresponding $\sqrt{\chi^2_{red}}$. Using a single component model and assuming the fitted b parameter value to be the same for all J−levels, the best fit converges to $\Delta\mu/\mu$ = (4.8 ± 4.2) ppm with an overall χ^2_{red} of 1.60. As VPFIT errors purely reflect the statistical errors the larger error from the bootstrap method can be used to quantify the associated systematic errors by considering the quadratic sum of the two errors. In this case we find it to be 4.4 ppm. We apply the same analysis to the combined spectrum made of CPL generated 1-d spectra. For this model we find $\Delta\mu/\mu$ = (9.1 ± 4.7) ppm for such a combined spectrum. The two values differ by ~ 1-σ. Therefore systematic errors as large as 4.3 ppm can be produced if using the final 1-d spectra generated by CPL. Allowing b parameters of different J levels to be different, the best-fitting $\Delta\mu/\mu$ is of (5.5 ± 4.3) ppm with a slightly better AICC value. In this case the comparison of the estimated error from the bootstrap method (second line in Table 1) suggests a systematic error of 4.0 ppm. We also consider two velocity component models. We were able to obtain a consistent result only when the Doppler parameter is different for different J-levels. The two components are separated by (0.19 ± 0.11) km s^{-1}. We find $\Delta\mu/\mu$ = (6.5 ± 4.3) ppm. The 2 component fit using shift-corrected data yields larger $\Delta\mu/\mu$ by ~ 2–3 ppm.

It is clear from Table 1 that while there is a marginal improvement in the χ^2_{red} and AICC in the 2 component model, the final results are very much consistent with one another. Moreover, the best model is the two-component model for both shift-corrected and not corrected spectra. Therefore, we choose the two component H_2 fit as the best model of the data. As in Rahmani et al. (2013) we quote the final error in $\Delta\mu/\mu$ including the systematic error obtained above and the statistical error given by VPFIT. Therefore, we consider the best measurement to be $\Delta\mu/\mu$ = (7.4 ± 4.3$_{\rm stat}$ ± 4.4$_{\rm sys}$) ppm.

Table 1. $\Delta\mu/\mu$ estimations using H_2 lines in the z_{abs} = 2.6586 H_2-bearing cloud toward Q 0643−5041. The quoted errors in $\Delta\mu/\mu$ come mainly from statistical errors.

			$\Delta\mu/\mu \times 10^6$					
			1 component			shift-corrected		
Fit	Error	b	$\Delta\mu/\mu$	χ^2_{red}	AICC	$\Delta\mu/\mu$	χ^2_{red}	AICC
l-b-l	bootstrap	tied	5.0 ± 6.1	1.57	...	8.1 ± 6.6	1.53	...
l-b-l	bootstrap	free	4.6 ± 5.9	1.55	...	7.6 ± 6.4	1.51	...
VPFIT	weighted	tied	4.8 ± 4.2	1.58	7318	5.9 ± 4.2	1.57	7299
VPFIT	weighted	free	5.5 ± 4.3	1.58	7301	6.7 ± 4.2	1.55	7204
			2 components			shift-corrected		
VPFIT	weighted	free	6.5 ± 4.3	1.57	7253	7.4 ± 4.3	1.53	7150

5. Conclusion

At present, measurements of $\Delta\mu/\mu$ using H_2 are limited to 6 H_2-bearing DLAs at $z \geq 2$ (see Albornoz Vásquez et al. 2013, and references therein). All these measurements are consistent with null $\Delta\mu/\mu$ at the level of 10 ppm. Here we present a $\Delta\mu/\mu$ constraint using 14 ∼ 1 hour exposures of the quasar Q 0643−5041 taken with attached ThAr calibrations having an H_2 absorption at z_{abs}= 2.6586. We selected 81 H_2 lines suitable for $\Delta\mu/\mu$ measurements. The best model of the H_2 absorption profile is a two velocity component model with untied Doppler parameters between different rotational levels, with $\Delta\mu/\mu = (7.3 \pm 4.3_{stat} \pm 4.1_{sys})$ ppm. Our result is consistent with no variation of μ over the last 11.2 Gyr. Fig. 2 summarizes $\Delta\mu/\mu$ measurements based on different approaches at different redshifts. Our new measurement is consistent with all the other measurements based on H_2 lines. However, we also note that like the majority of other studies our $\Delta\mu/\mu$ is positive although consistent with zero.

It seems rather difficult to go much beyond our analysis on the variation of μ with UVES data. Indeed, systematic drifts in wavelength calibration over the whole blue arm of UVES can only be unveiled by absolute reference observations (of asteroids or an iodine cell, for example) in the same conditions as science observations to correct for instrumental misbehaviours. Such a systematic effect could be the origin of the preferred positive value of $\Delta\mu/\mu$ seen in this and other similar works.

Acknowledgements. This research was supported by the Agence Nationale pour la Recherche under Prog. ANR-10-BLAN-510-01. R. S. and P. P. J. gratefully acknowledge support from the Indo-French Centre for the Promotion of Advanced Research (Centre Franco-Indien pour la Promotion de la Recherche Avancée) under contract No. 4304-2. H. R. would like to thank the Institute for Research in Fundamental Sciences (IPM, Tehran) for hospitality and providing facilities during his visit in August-September 2013.

References

Albornoz Vásquez D., et al. 2013, submitted to A&A
Bagdonaite, J., et al. 2013, Science, 339, 46
Balashev, S. A., et al. 2011, MNRAS, 418, 357
Dekker, H., et al. 2000, Proc. SPIE, 4008, 534
D'Odorico, S., et al. 2000, Proc. SPIE, 4005, 121
King, J. A., et al. 2008, Phys. Rev. Lett., 101, 4
King, J. A., et al. 2011, MNRAS, 417, 3010
Murphy, M. T., Flambaum, V. V., Muller, S., & Henkel, C. 2008, Science, 320, 1611
Malec, A. L., et al. 2010, MNRAS, 403, 1541
Mohr P. & Taylor B. 2000, Rev.Mod.Phys., 72, 351
Noterdaeme, P., et al. 2007, A&A, 474, 393
Noterdaeme, P., Ledoux, C., Petitjean, P., & Srianand, R. 2008a, A&A, 481, 327
Rahmani, H., et al. 2013, MNRAS, 425, 556
Rahmani, H., et al. 2013, `arXiv:1307.5864`
Srianand, R., et al. 2010, MNRAS, 405, 1888
Thompson, R. I. 1975, Astrophys. Lett., 16, 3
Ubachs, W., Buning, R., Eikema, K. S. E., & Reinhold, E. 2007, J. Molec. Spec., 241, 155
Wendt M. & Molaro P. 2012, A&A, 541, 69